JOURNAL OF MORPHOLOGY 271:340–352 (2010)

Functional Morphology of the Radialis Muscle in Shark Tails

Brooke E. Flammang*

Museum of Comparative Zoology, Harvard University, Cambridge, Massachusetts 02138

ABSTRACT The functional morphology of intrinsic caudal musculature in sharks has not been studied previously, though the kinematics and function of body musculature have been the focus of a great deal of research. In the tail, ventral to the axial myomeres, there is a thin strip of red muscle with fibers angled dorsoposteriorly, known as the radialis. This research gives the first anatomical description of the radialis muscle in sharks, and addresses the hypothesis that the radialis muscle provides postural stiffening in the tail of live swimming sharks. The radialis muscle fibers insert onto the deepest layers of the stratum compactum, the more superior layers of which are orthogonally arrayed and connect to the epidermis. The two deepest layers of the stratum compactum insert onto the proximal ends of the ceratotrichia of the caudal fin. This anatomical arrangement exists in sharks and is modified in rays, but was not found in skates or chimaeras. Electromyography of the caudal muscles of dogfish swimming steadily at 0.25 and 0.5 body lengths per second (L s^{-1}) exhibited a pattern of anterior to posterior activation of the radialis muscle, followed by activation of red axial muscle in the more anteriorly located ipsilateral myomeres of the caudal peduncle; at 0.75 L s^{-1}, only the anterior portion of the radialis and white axial muscle of the contralateral peduncular myomeres were active. Activity of the radialis muscle occurred during periods of the greatest drag incurred by the tail during the tail beat and preceded the activity of more anteriorly located axial myomeres. This nonconformity to the typical anterior to posterior wave of muscle activation in fish swimming, in combination with anatomical positioning of the radialis muscles and stratum compactum, suggests that radialis activity may have a postural function to stiffen the fin, and does not function as a typical myotomal muscle. J. Morphol. 271:340–352, 2010.

KEY WORDS: dogfish; swimming; caudal fin; intramuscular pressure; stratum compactum; collagen

INTRODUCTION

Locomotion of sharks has been studied extensively, particularly whole body kinematics (Lowe, 1996; Donley et al., 2005) and muscle physiology (Bone, 1966; Bone et al., 1978; Bone et al., 1986; 1999; Donley and Shadwick, 2003). Like other fishes, the axial myotomes of sharks have separate sections of slow-oxidative (red) and fast-glycolytic (white) muscle fibers, which are active at lower and higher speeds, respectively (Bone, 1966; Bone et al., 1978; Donley and Shadwick, 2003; Donley et al., 2005; Sepulveda et al., 2005). These axial myomeres extend the length of the vertebral column, ending in the dorsal lobe of the caudal fin in most sharks. Caudal fin morphology (Affleck, 1950; Alexander, 1965; Lingham-Soliar, 2005), kinematic, and hydrodynamic research (Alexander, 1965; Simons, 1970; Ferry and Lauder, 1996; Wilga and Lauder, 2002, 2004) has focused primarily on external morphology with little investigation of the functional internal anatomy of the tail fin.

The caudal fin of sharks is the most prominent control surface for locomotion, controlling the angle of attack of the fin by leading the tail beat with the dorsal tip of the caudal fin (Ferry and Lauder, 1996). This produces a downward posteriorly oriented jet, creating thrust in the forward and upward direction (Ferry and Lauder, 1996; Wilga and Lauder, 2002, 2004). Control of the angles of attack of the dorsal and ventral lobes of the caudal fin can be accomplished in two ways: by rotating a completely stiff fin into the appropriate angle or by modulating stiffness and local motor control. In support of the first possibility, high aspect ratio fins are only useful if they are stiff, otherwise they contribute to drag (Nursall, 1958). However, torsion of the caudal peduncle is impeded by the orthogonal helices of collagen fibers that lie in the shark skin (Motta, 1977; Wainwright et al., 1978), making rotation of a fin unlikely. In contrast to teleost fishes, which have an intricate array of intrinsic caudal muscles that modulate fin ray orientation in three-dimensional range of motion (Flammang and Lauder, 2008,

Contract grant sponsors: NSF IGERT, The Barbour fund (MCZ), Friday Harbor Marine Science Fellowship, Robert A. Chapman Memorial Scholarship.

*Correspondence to: Brooke E. Flammang, Museum of Comparative Zoology, Harvard University, Cambridge, MA 02138.
E-mail: bflammang@oeb.harvard.edu

Received 20 March 2009; Revised 2 July 2009;
Accepted 30 July 2009

Published online 13 October 2009 in
Wiley InterScience (www.interscience.wiley.com)
DOI: 10.1002/jmor.10801

2009), sharks possess only a single strip of red muscle deep to the dermis and separate from the axial myomeres, described as the radialis (Alexander, 1965). From experiments using the tails of dead sharks to try to determine lift produced during swimming, Alexander (1965) suggested that sharks actively modify the angle of attack of the ventral lobe of the tail, possibly by using the radialis muscle. Aside from Alexander's (1965) hypothesis, the action of the radialis muscle or its activity during steady swimming in controlling tail fin angle of attack, shape modulation, or stiffness has not previously been investigated. Because the radialis muscle is located in the dorsal lobe of the tail of sharks and Alexander's (1965) experiments with tails of dead sharks showed the dorsal lobe to be dragging behind as it was moved through the water, it is hypothesized that action of the radialis muscle in a live shark is to control stiffness of the tail during steady swimming. To address this hypothesis, a detailed anatomical description of the radialis muscle is needed. The goal of this research is to provide a comparative anatomical description of the radialis muscle in a diversity of chondrichthyans for the first time and to determine how the activity of the radialis muscle correlates with the kinematics of the caudal fin in swimming sharks. If the radialis muscle is used for tail stiffening and not for kinematic modulation, this should be reflected in electromyographic recordings of the activation patterns of the radialis. Controlled stimulation experiments of the radialis muscle should also produce no discernable fin shape modification. Lastly, if acting in a postural role, the activity patterns of the radialis muscle should not change in response to increased swimming speeds as is typically seen in the activity patterns of axial muscles.

MATERIALS AND METHODS

Animals

Specimens used for anatomical dissection were borrowed from the Museum of Comparative Zoology (Harvard University). Representatives from eleven different families of cartilaginous fishes (Chondrichthyes) were used for comparative analysis of caudal muscle morphology. Examined sharks included Alopiidae (*Alopias vulpinas*, thresher shark; $n = 1$), Centrophoridae (*Centrophorus* sp., gulper shark; $n = 1$), Cetorhinidae (*Cetorhinus maximus*, basking shark; $n = 1$), Lamnidae (*Isurus oxyrhincus*, mako shark; $n = 1$), Scyliorhinidae (*Parmaturus xaniurus*, filetail catshark, $n = 1$ and *Cephaloscyllium ventriosum*, swellshark; $n = 1$), Squalidae (*Squalus acanthias*, spiny dogfish; $n = 4$), Squatinidae (*Squatina californica*, angel shark; $n = 1$), Triakidae (*Triakis semifasciata*, leopard shark, $n = 1$, *Mustelus henleii,* $n = 1$ and *M. canis*, $n = 1$, smoothhound sharks). Batoids were represented by Narcinidae (*Narcine brasiliensis*, electric ray; $n = 1$) and Rajiidae (*Leucoraja erinacea*, little skate; $n = 1$). *Chimaera monstrosa*, giant chimaera ($n = 1$), was also included as an outgroup holocephalan representative. Total length of the body, length of the dorsal tail lobe, length of the radial muscle, muscle fiber length, and muscle fiber angle were determined for a representative of each species. Dorsal lobe length, measured from the dorsal tip of the tail (point 1, Fig. 1A) to the caudal peduncle (point 5, Fig. 1A) was used to standardize radialis muscle morphometrics for comparison among species, as the radialis muscle was confined within the dorsal lobe of the tail in most species and size of the radialis relative to total tail length is physiologically relevant to the action of the radialis muscle within the tail.

Live adult spiny dogfish (*Squalus acanthias* Linnaeus) were purchased from the Marine Resource Center at Woods Hole Oceanographic Institute (Woods Hole, Massachusetts) and kept in a 2,400 l circular tank at 16°C with 12:12 h light:dark cycles and fed three times weekly. The week before experiments, sharks were trained daily to swim in the central region of the flow tank, away from the walls, for 1–2 h per day. During training, the goal was for sharks to maintain speed and position for 1 min and sharks seldom swam at or above 1.0 body length per second (L s^{-1}) for the full duration of 1 min. A total of five spiny dogfish (3 males and 2 females) were used for electromyographic and kinematic study (59.2 ± 10.4 cm total length (L), mean ± s.d.), and all individuals were confirmed as mature by postmortem dissection. One additional male spiny dogfish (64 cm L) was used for muscle stimulation. Physiological cross-sectional area (PCA) was calculated using a muscle density of 1.056 g cm^{-2} (Lowndes, 1955) from four adult spiny dogfish that died in captivity of natural causes. Comparisons of PCA among all species examined were not possible as specimens were preserved and accurate muscle masses could not be obtained.

Electrical Stimulation Experiment

Electrical stimulation of the radialis muscle was performed to initiate a muscle contraction and determine what changes in tail shape may be occurring without the confounding effect of hydrodynamic pressures incurred during swimming. A lethal dose of potassium hydroxide-buffered tricaine methanesulfonate (MS222) was administered to one individual and electromyographic electrodes were implanted into the posterior and anterior ends of the radialis muscle on both the left and right sides. The free ends of the electrodes were attached to a Grass S44 electrical stimulator. The tail was completely submerged and the dorsal and ventral tips of the tail were suspended in the water column with no contact to the tank sides. Muscles were stimulated at each region separately, unilaterally (anterior and posterior electrodes simultaneously), and bilaterally (all electrodes simultaneously) at 10–20 V for 1 s duration at 10–30 pulses s^{-1} with a 1 ms delay between pulses. Stimulation experiments were captured at 30 frames per second using a video camera (Sony Digital Handycam DCR-TRV38). To quantitatively evaluate the extent of tail flexion, the dorsal tip of the tail was designated as 0°, the ventral tip of the tail was designated as 180°, and flexion of either fin lobe was considered to be approaching 90° (midline) on either side.

Electromyography

Sharks were anesthetized using MS222 and were ventilated via an oral cannula throughout the procedure using water oxygenated by an aquarium air pump (Flammang and Lauder, 2008, 2009). Following electrode placement, sharks were allowed to fully recuperate in the flow tank for a minimum of three times the duration they were under anesthesia before any experimentation began.

To make electrodes, 2.5 m lengths of 0.05 mm diameter bifilar Teflon-coated steel wire (California Fine Wire, Grover Beach, CA) were split 1 mm from the end and 0.5 mm of the tip of one wire was removed. Insulation was removed from a 0.5 mm section of each prong, and the electrode tips were bent back and apart from each other, into a hook-shape. Subcutaneous surgical implantation in the tail muscles was achieved by threading the electrode through a 26-guage needle. Electrode

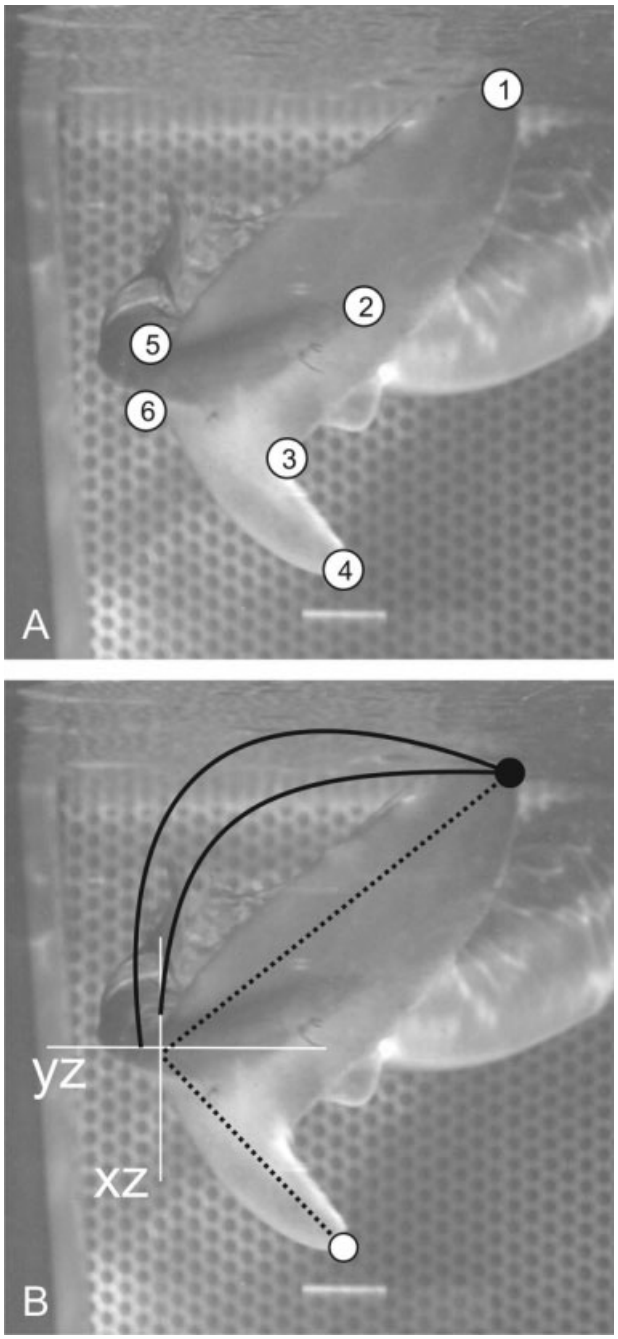

Fig. 1. Posterior view image of shark swimming in flow tank with digitized points and measured angles superimposed. **A:** Six points on the tail of the shark that were digitized for kinematic analysis, explanation in text. **B:** Illustration of how the angle of orientation was determined for the dorsal tail tip, using the cosine rule to relate the points to each other in three dimensions, relative to the transverse plane defined by *xz*, a straight line through points 5 and 6, and *yz*, perpendicular to the long axis of the body. The same method was applied for the ventral tail tip.

construction was standardized so as to minimize signal variation.

A total of eight electrodes were placed in the white and red muscle of the caudal peduncle and fin. Specifically targeted were: a) the white muscle of the axial myomere on the left (LW) and right sides (RW) of the caudal peduncle at 0.78 body length (L), b) the thin lateral strip of red muscle in the axial myomeres on the left (LR) and right (RR) of the caudal peduncle, also at 0.78 L, c) the anterior end of the radialis muscle above the middle of the ventral lobe of the fin at 0.84 L on the left (LAR) and right (RAR) sides, and d) the posterior end of the radialis muscle midway between the fork of the tail and the end of the vertebral column at 0.90 L on the left (LPR) and right (RPR) sides. The electrodes were held in place at the insertion sites and anterior to the caudal peduncle and second dorsal fin, to ensure swimming motions would not contact the wires, using 4/0 silk black braided sutures and cyanoacrylate.

Electromyographic signals were digitally recorded using an ADInstruments PowerLab/16SP analog-to-digital converter and Chart 5.5.5 software (ADIntruments, Colorado Springs, CO) at a sampling rate of 4 kHz, after being amplified by a factor of 5,000 using Grass model P511 K amplifiers with a 60 Hz notch filter and high- and low-bandpass filter settings of 100 Hz and 3 kHz, respectively. Electromyographic signals were recorded for a total of five sharks each swimming steadily at 0.25, 0.5, and 0.75 L s^{-1} for a minimum of three consecutive tail beats at each speed. Following experiments, sharks were euthanized and preserved in formalin so that electrodes could be dissected out to verify placement.

Kinematic Protocol

Kinematic data were gathered while sharks swam in the 80 cm × 26 cm × 26 cm working area of a 600 l recirculating tank (Flammang and Lauder, 2008, 2009). Lateral, posterior, and ventral views of the sharks swimming steadily at 0.25, 0.5, and 0.75 L s^{-1} were recorded using three high-speed digital video cameras (Photron, San Diego, CA) with 1,024 by 1,024 pixel resolution at 250 frames s^{-1}, which were synchronized with electromyographic (EMG) data collection. The three video positions were calibrated in three dimensions using direct linear transformation of a custom 40-point calibration object and digitized using a program written for MATLAB R2007a (MathWorks, Natick, MA) by T. Hedrick (Hedrick, 2008). Six points were digitized on the caudal fin for kinematic analysis of each tail beat: 1) the posterior-most tip of the dorsal lobe, 2) the posterior-most point of the cone of axial myomeres that extend into the tail, 3) the fork of the tail, 4) the posterior-most point of the ventral lobe, 5) the dorsal origin of the caudal fin at the caudal peduncle, and 6) the ventral origin of the caudal fin at the caudal peduncle (Fig. 1A). Steady swimming was defined as a minimum of three continuous tail beats without lateral maneuvers or acceleration. As high-speed video was synchronized with EMG recording, and it was hypothesized that different muscle groups (e.g., red or white) would be active at different speeds, all five sharks swam steadily at three different speeds: 0.25, 0.5, and 0.75 L s^{-1}. Given the mean size of sharks used this represented swimming speeds of ~15, 30, and 45 cm s^{-1}. These speeds were chosen because they resembled observed natural swimming patterns and because swimming at speeds equal to or greater than 1.0 L s^{-1} tended to have intermittent acceleration kicks.

Two kinematic variables were used to describe the actions of the caudal fin: amplitude of the tail beat and angle of the dorsal and ventral lobe relative to the long axis of the body. Amplitude was determined by tracking the mean lateral excursion of the dorsal tip of the tail (point 1) throughout the tail beat using three-dimensional positioning. The angle (°) of the dorsal (point 1) and ventral (point 4) tips of the caudal fin lobes relative to the transverse plane at the junction of the caudal fin with the axial body at the peduncle (defined by two reference dimensions: *xz*, a straight line through points 5 and 6, and *yz*, perpendicular to the sagittal plane of the body) was determined using the cosine rule applied to a basic algebraic function to relate the points to each other in three dimensions (Fig. 1B). The three-dimensional angles of point 1 and point 4 are the equiva-

lent of the dorsal tip of triangle A and ventral tip of triangle G used by Ferry and Lauder (1996) and help to standardize the tail fin orientation with respect to the body orientation.

Data Analysis

Only electromyographic recordings that corresponded with video sequences in which all three camera views of the shark displayed steady swimming for a minimum of three consecutive tail beats were used for analysis of muscle activity. Then, the middle tail beat of each sequence of three or more consecutive tail beats was analyzed for muscle activity and kinematics, to ensure steady swimming and avoid pseudoreplication. Because of these strict criteria for analysis, a large number of video and EMG sequences were discarded and a total of twenty-eight tail beat sequences from five sharks swimming steadily were used for kinematic and EMG analyses: 10 at 0.25 L s^{-1} (n = 3, 3, 2, 1, 1 from each of the five individual sharks), eight at 0.5 L s^{-1} (n = 2, 2, 2, 1, 1), and 10 at 0.75 L s^{-1} (n = 3, 2, 2, 1, 2). Because of the terminal nature of these experiments and as there was no statistical difference among individuals (F_{ANOVA} = 0.942, $F_{0.05(1)4,14}$ = 3.11, $P > 0.25$), using additional individuals was not justified. The EMG results were filtered using a high and low bandpass filter, rectified and integrated, and duration, relative onset, and intensity of muscle activity were digitized using Chart 5.5.5 software. Muscle activity duration was standardized to the total duration of the tail beat. Onset of muscle activity was defined relative to the maximum lateral excursion of the dorsal tip of the tail to the shark's right side as determined by the digitized videos. Intensity of muscle activity was defined as the integral of the rectified EMG burst. Analysis of variance (ANOVA) was used to determine if duration, onset, or intensity of muscle activity was statistically different among swimming speeds (Systat 11.0).

RESULTS

Caudal Fin Anatomy

Deep to the epidermis in the caudal fin of spiny dogfish are five layers of orthogonally arrayed subdermal collagen fibers known as the stratum compactum. Collagen fibers of all layers of the stratum compactum are oriented at approximately ±45° from the longitudinal axis of the shark. The first, most superficial layer of the stratum compactum is oriented at a diagonal, anteroventrally to posterodorsally, and anchored firmly to the epidermis. Each deeper layer of collagen fibers is orthogonal to the layer above it. Between the third and fourth layers is a single long bundle of collagen fibers which runs anteroposteriorly, directly beneath the lateral line. The fourth layer of subdermal collagen fibers is tightly interconnected with the fifth layer and covers the radialis muscle, inserting onto the proximal ends of the ceratotrichia ventral to the vertebral column.

The radialis muscle is a thin strip of red muscle which lies ventral to the axial musculature of the caudal fin (see Fig. 2) and in spiny dogfish had a mean PCA of 0.513 cm^2 and average muscle fiber length 6.82 ± 1.05 mm (n = 4). This muscle originates at the anterior margin of the ventral lobe of the caudal fin and tapers posteriorly towards the penultimate vertebra. The individual muscle fibers originate on the hemal arches of the caudal vertebrae and insert posteriorly into the fifth and deepest layer of orthogonally arrayed collagen fibers. This fifth layer of subdermal collagen fibers inserts onto the proximal ends of the ceratotrichia which are dorsal to the vertebral column (see Fig. 2).

The axial myomeres in the caudal fin are a series of interlocking anteriorly and posteriorly oriented cones of muscle, and taper toward the penultimate vertebra deep to the radialis muscle and the fifth layer of subdermal collagen fibers. The deepest cones of the axial myomeres insert onto the connective tissue covering the vertebral column.

Comparisons of fourteen species of cartilaginous fishes from eleven different families illustrated conservation of the anatomy of the radialis muscle and relative size of the radialis muscle with regards to the size of the tail, with notable phylogenetic exceptions (Table 1). There was no radialis muscle present in chimaera (*Chimaera monstrosa*) or the skate (*Leucoraja erinacea*); only the white axial muscle was present in the caudal fin. However, the other batoid representative, the electric ray (*Narcine brasiliensis*), had a radialis muscle that extended anteriorly along the ventral surface of the tail, ending at the same point on the body as the anterior origin of the first dorsal fin. The radialis muscle in the angel shark (*Squatina californica*) also extended anteriorly, but only to the same point on the body as the posterior insertion of the second dorsal fin. The spiny dogfish had the shortest radialis muscle relative to the length of its dorsal lobe. Muscle fiber length for most sharks was 0.051–0.061% of dorsal lobe length, with the exception of catsharks (0.028–0.036% dorsal lobe length), the mako shark (0.09% dorsal lobe length), and the thresher shark (0.014% dorsal lobe length). Angle of radialis muscle fibers to the long axis of the body was between 43 and 59° for all species.

Electrical Stimulation

Stimulation of the radialis muscle in spiny dogfish produced little to no change in tail shape or orientation in all cases. When only one of the four implanted electrodes was activated, there was no change in orientation of the dorsal or ventral tail tip. With unilateral stimulation, where both the anterior and posterior ends of the radialis muscle were stimulated on the same side, flexion of the dorsal tail tip of 5–7° was observed on the ipsilateral side with no effect on the ventral tail tip. When the radial muscles were bilaterally stimulated, no flexion of the dorsal or ventral tail tips was observed.

Electromyographic and Kinematic Analyses

Electromyographic recordings illustrated a consistent pattern of anterior to posterior radialis

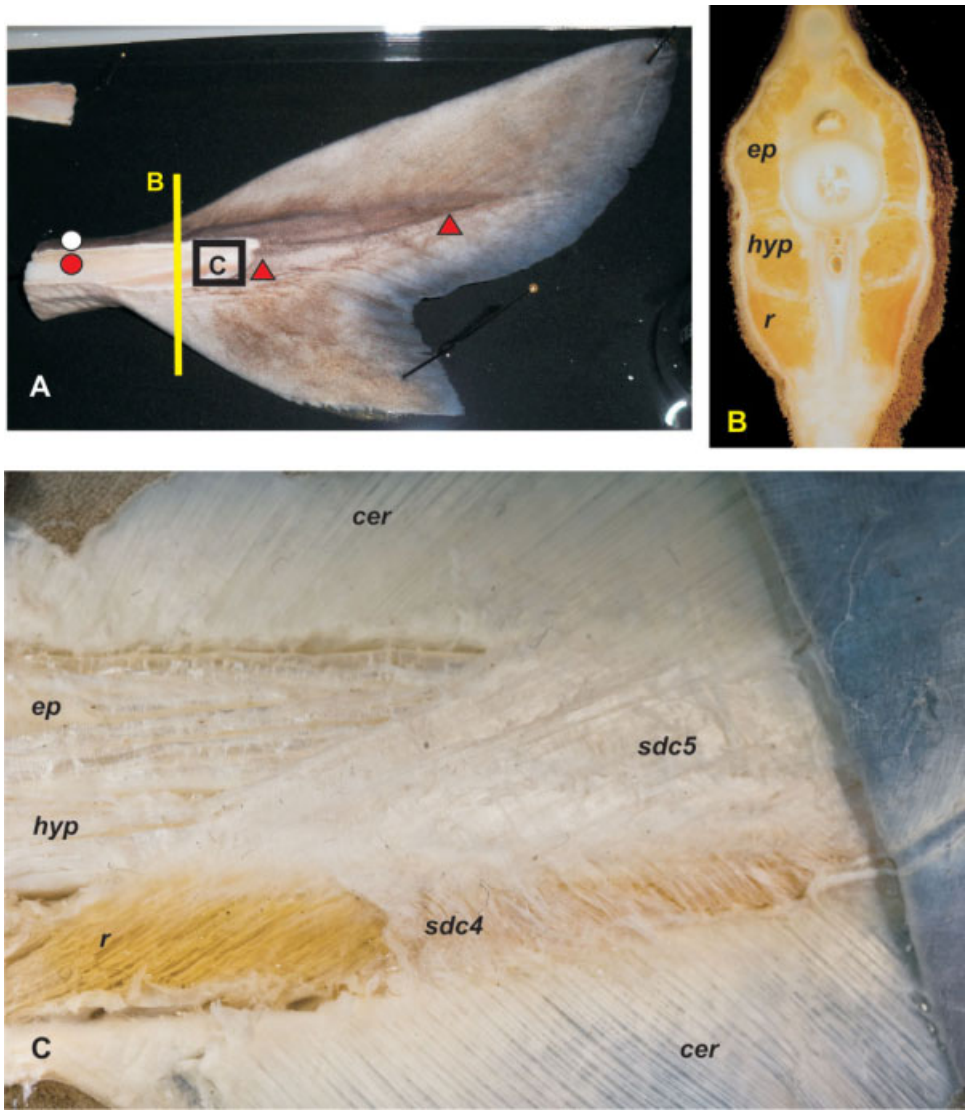

Fig. 2. Partial dissection of the radialis muscle of a spiny dogfish (*Squalus acanthias*) to show the location of the muscle in the tail fin. **A:** Photograph of the caudal fin. Electrodes for electromyographic recording were implanted in the red (red circle) and white (white circle) axial muscle of the caudal peduncle and anterior and posterior regions of the radialis muscle (red triangles). **B:** Cross-section of caudal fin at the plane designated in A in yellow; ep, epaxial musculature; hyp, hypaxial musculature; r, radialis muscle. **C:** Image of inset in A, taken with a polarizing filter, in which the three superficial layers of subdermal collagen fibers and skin have been reflected back to illustrate the insertion of the individual muscle fibers into the fifth layer of subdermal collagen fibers, *sdc5*, and of these collagen fibers onto the proximal ends of the dorsal ceratotrichia, *cer*. Orthogonal to, and directly above the radialis muscle is the fourth layer of subdermal collagen fibers, *sdc4*, which insert into the ventral ceratotrichia. [Color figure can be viewed in the online issue, which is available at www.interscience.wiley.com.]

activation in spiny dogfish (see Fig. 3), which was observed during all speeds. The left anterior radialis was active just after right maximum lateral excursion of the dorsal tip of the tail, as the tail began to move to the left. The left red axial muscle of the caudal peduncle was active after the more posteriorly located left anterior end of the radialis muscle. The activity of the radialis left posterior end ended just before left maximum lateral excursion.

Radialis muscle activity duration, relative onset from respective sides of maximum excursion, and EMG burst intensity were not statistically different among anterior and posterior ends or right and left muscles (Fig. 4; $P = 0.383$); however, the posterior ends of the radialis muscles were not active during swimming at 0.75 L s^{-1}. The duration of radial muscle activity was not significantly different from duration of red axial muscle tissue (Fig. 4A; $t_{0.05(2),34}$, $P = 0.125$). The red axial musculature was active only at swimming speeds of 0.25 and 0.5 L s^{-1}, except for four isolated, anomalous beats from one individual swimming at 0.75 L s^{-1}, where it was active for the exact same

TABLE 1. Comparative morphometrics of the radialis muscle from one representative each of eleven different species of elasmobranches

Species	Total length (cm)	Dorsal lobe length (cm)[a]	Radialis length (cm)[b]	Muscle fiber length (mm)[b,c]	Muscle fiber angle (°)[c]	Radialis location in tail
Thresher shark (*Alopias vulpinas*)	232	95.3 (41.1)	93.0 (97.6)	12.87 ± 1.41 (0.014)	51.8 ± 6.8	
Gulper shark (*Centrophorus* sp.)	156	29.4 (18.8)	23.2 (78.9)	16.28 ± 0.87 (0.055)	46.4 ± 2.0	
Basking shark (*Cetorhinus maximus*)	435	79.8 (18.3)	69.4 (87.0)	40.55 ± 8.68 (0.051)	59.4 ± 7.2	
Mako shark (*Isurus oxyrhincus*)	57.8	13.0 (22.5)	11.8 (90.8)	11.75 ± 1.75 (0.090)	52.0 ± 4.2	
Filetail catshark (*Parmaturus xaniurus*)	42.1	9.0 (21.4)	8.2 (91.1)	2.57 ± 0.097 (0.028)	51.1 ± 2.6	
Swell shark (*Cephalloscyllium ventriosum*)	28.7	7.9 (27.5)	6.1 (77.2)	2.88 ± 0.12 (0.036)	50.6 ± 5.9	
Spiny dogfish (*Squalus acanthias*)	57.4	12.4 (21.6)	7.1 (57.2)	6.82 ± 1.05 (0.055)	42.9 ± 3.1	
Smooth hound (*Mustelus canis*)	62.5	11.0 (17.6)	8.5 (77.3)	6.72 ± 0.92 (0.061)	45.1 ± 1.8	
Leopard shark (*Triakis semifasciata*)	32.2	7.5 (23.3)	6.3 (84.0)	4.32 ± 0.55 (0.058)	45.4 ± 1.5	
Angel shark (*Squatina californica*)	111.8	14.2 (12.7)	26.1 (183.8)	14.74 ± 1.27 (0.104)	50.5 ± 4.0	
Electric ray (*Narcine brasiliensis*)	31.6	3.3 (10.4)	8.9 (269.7)	5.32 ± 0.46 (0.161)	55.4 ± 3.4	

[a]Dorsal lobe length percentage of total length is in parentheses.
[b]Radialis muscle length and muscle fiber length percentages of dorsal lobe length are in parentheses.
[c]Mean ± S.E.M. of five measurements of radialis muscle fiber length and angle from the long axis of the body, from approximately equally-spaced locations along the entire length of the radialis muscle.

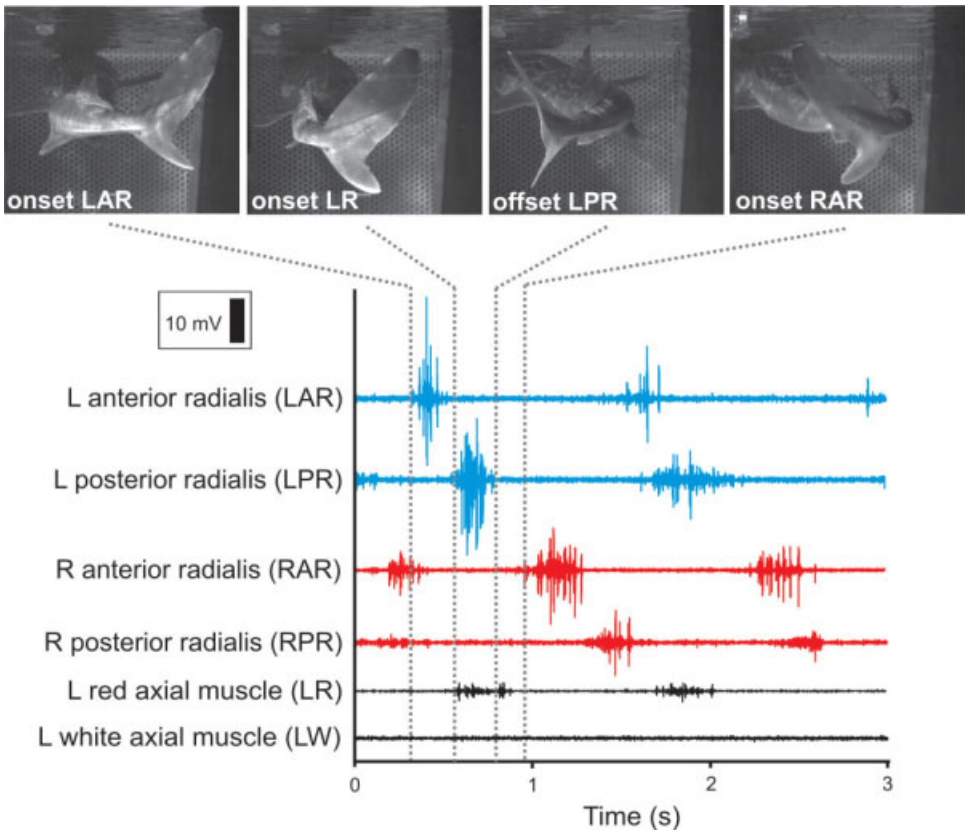

Fig. 3. Electromyographic recordings of the left (blue) anterior and posterior radialis, right (red) anterior and posterior radialis, and left red and white axial muscle of the caudal peduncle (black) of a spiny dogfish (*Squalus acanthias*) swimming steadily at 0.5 L s^{-1}. Above are corresponding posterior-view images from the high-speed video, which have been reversed to account for mirror-imaging and cropped to frame the caudal fin. [Color figure can be viewed in the online issue, which is available at www.interscience.wiley.com.]

time as the white axial muscle. The white axial musculature was active only at 0.75 L s^{-1} and for a significantly shorter period, a third of the duration as the red axial musculature ($t_{0.05(2),26}$, $P < 0.01$). There was a significant decrease in muscle activity duration with increasing swimming speed ($P < 0.001$). The relative onset of the left red axial musculature and ipsilateral radialis muscle was significantly different from the onset of the white axial musculature and contralateral right radialis muscle (Fig. 4B; $t_{0.05(2),27}$, $P < 0.01$). No difference in EMG burst intensity was found among radialis and red axial muscle sites, but there was a significant threefold difference in burst intensity of the white axial muscle when compared with all others (Fig. 4C; $P < 0.001$).

The lateral excursion of the dorsal tip of the caudal fin in spiny dogfish was approximately 8 cm from the midline among all speeds (see Fig. 5). Swimming at 0.25 L s^{-1}, sharks had a mean tail beat frequency of 0.74 ± 0.02 Hz. The velocity of the dorsal tip of the tail was greatest after the tail passed behind the shark at 35 and 85% of the tail beat cycle. Mean maximum velocity of the dorsal tip of the tail was 32.6 ± 1.34 cm s^{-1} (Fig. 5A). Radialis muscle activity began before maximum lateral excursion during swimming at 0.5 L s^{-1}, but earlier than at 0.25 L s^{-1} (Fig. 5B). Mean tail beat frequency at 0.5 L s^{-1} was 0.82 ± 0.04 Hz. Mean maximum velocity of the dorsal tip of the tail at 0.5 L s^{-1} was 44.1 ± 6.12 cm s^{-1} and occurred at mid-stroke, just as the tail passed behind the shark at 25 and 75% of the tail beat. During steady swimming at 0.75 L s^{-1}, the anterior portions of the radialis were active longer and later in the tail beat (Fig. 5C). As was also shown in Figure 3, the white axial muscle was active coincident with the contralateral radialis muscle and no red axial muscle activity was detected at this higher speed. Mean tail beat frequency was 1.08 ± 0.11 Hz and maximum velocity of the dorsal tip of the tail was 44.4 ± 2.42 cm s^{-1} at 25 and 75% of the tail beat.

The angular positions of the dorsal and ventral tips of the caudal fin relative to the long axis of the body were in phase with each other throughout the tail beat, though the angle of the ventral lobe was less than half that of the dorsal lobe (see Fig. 6). During steady swimming at 0.5 L s^{-1} (Fig. 6A), the caudal fin was cupped into the direction

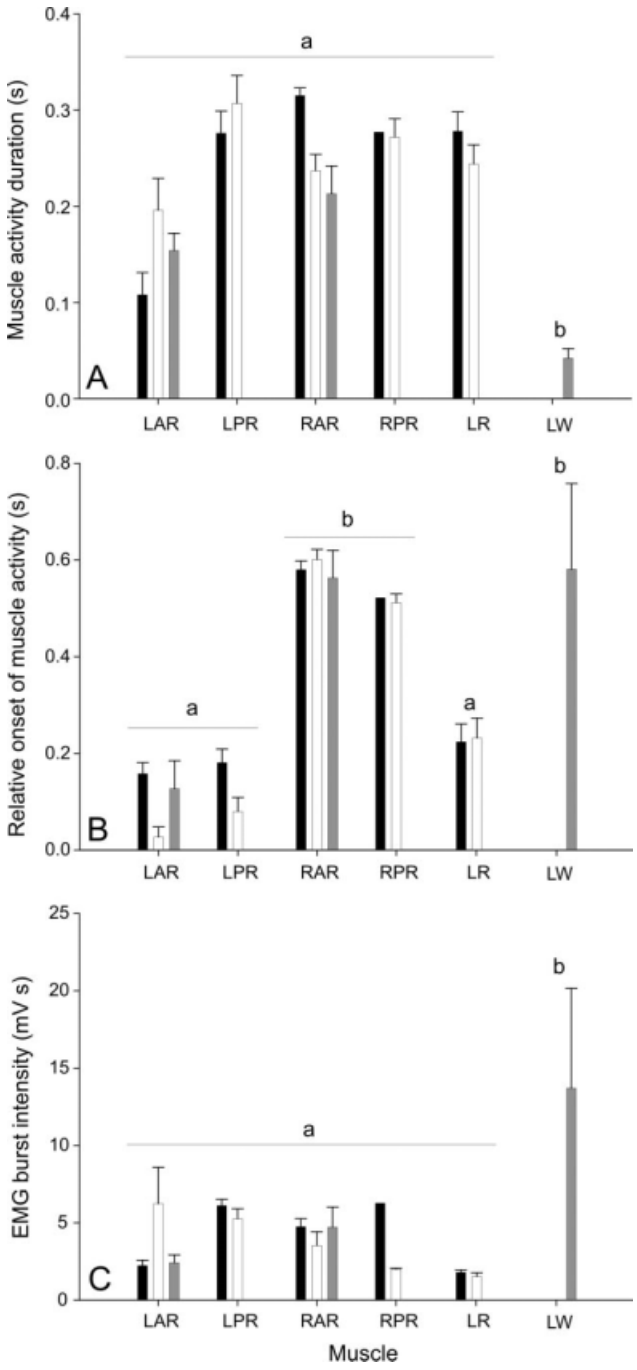

Fig. 4. Histograms of muscle duration (**A**), onset of muscle activity relative to the maximum right lateral excursion of the dorsal tail tip (**B**), and EMG burst intensity of caudal muscles (**C**) from all sequences of five individuals at 0.25 (black, n = 10), 0.5 (white, n = 8), and 0.75 L s^{-1} (gray, n = 10). Error bars indicate standard error of the mean. Muscle activity is shown for the left anterior radialis (LAR), left posterior radialis (LPR), right anterior radialis (RAR), right posterior radialis (RPR), left red axial musculature (LR), and left axial white muscle (LW). Bars with a common letter (e.g., a) were not statistically different from one another, but were significantly different from bars with other letters (ANOVA, $P < 0.01$). Bars absent for any muscle indicate that it was not active at that speed.

of travel and the greatest degree of cupping occurred approximately at mid-stroke, as the tail passed behind the shark. Conversely, during steady swimming at 0.75 L s^{-1} (Fig. 6B), the angle of the fin lobes remained relatively constant with almost no cupping, and exhibited a decrease in angle at the point of maximum excursion and change of direction of the tail fin.

DISCUSSION

The anatomy of the intrinsic caudal musculature in spiny dogfish seems to be ubiquitous among sharks and is notably different from the angel shark (Squatinidae) and skate and ray (batoid) conditions. Morphological results of dissection of the radialis in twelve families of sharks were consistent with Shirai's (1996) phylogenetic character 90, the location of the flexor caudalis, though the phylogeny itself has been refuted based on molecular evidence (Douady et al., 2003). Upon comparison with the molecular phylogeny produced by Douady et al. (2003), it appears the radialis muscle was not present in skates, first appeared in either rays or sharks, and extended anteriorly into the tail in the more recently derived angel sharks. The catsharks, which typically occupy a benthic habitat, had the shortest muscle fiber length relative to the size of their dorsal lobe and the fast-swimming mako shark had the longest relative muscle fiber length (Table 1). The radialis muscle in sharks is similar in anatomical position, but presumed not phylogenetically homologous, to the intrinsic caudal musculature of basal actinopterygian and teleost fishes (Gemballa, 2004; Flammang and Lauder, 2008, 2009).

Muscle Activity Patterns

Electromyographic activity in the red axial muscle as far posteriorly as 0.72 L has been recorded in leopard and mako sharks swimming up to speeds of 1.0 L s^{-1} (Donley and Shadwick, 2003; Donley et al., 2005), different from the change seen in the dogfish where muscle activity switched from red to white axial muscle at 0.75 L s^{-1}. However, the spiny dogfish differs ecologically from the mako shark in having a more benthic association with shorter bouts of continuous swimming, particularly in adults (Wetherbee et al., 1990; Masuda and Allen, 1993; Ebert, 2003; Domenici et al., 2004). The transition to rapid swimming using white muscle may occur more quickly in sedentary species, which have relatively less red muscle and a lower aerobic capacity (Greer-Walker and Pull, 1975; Dickson et al., 1993). Focally-innervated white muscle fibers propagate muscle action potentials and can inhibit nonpropagating, multi-innervated red muscle fibers at higher

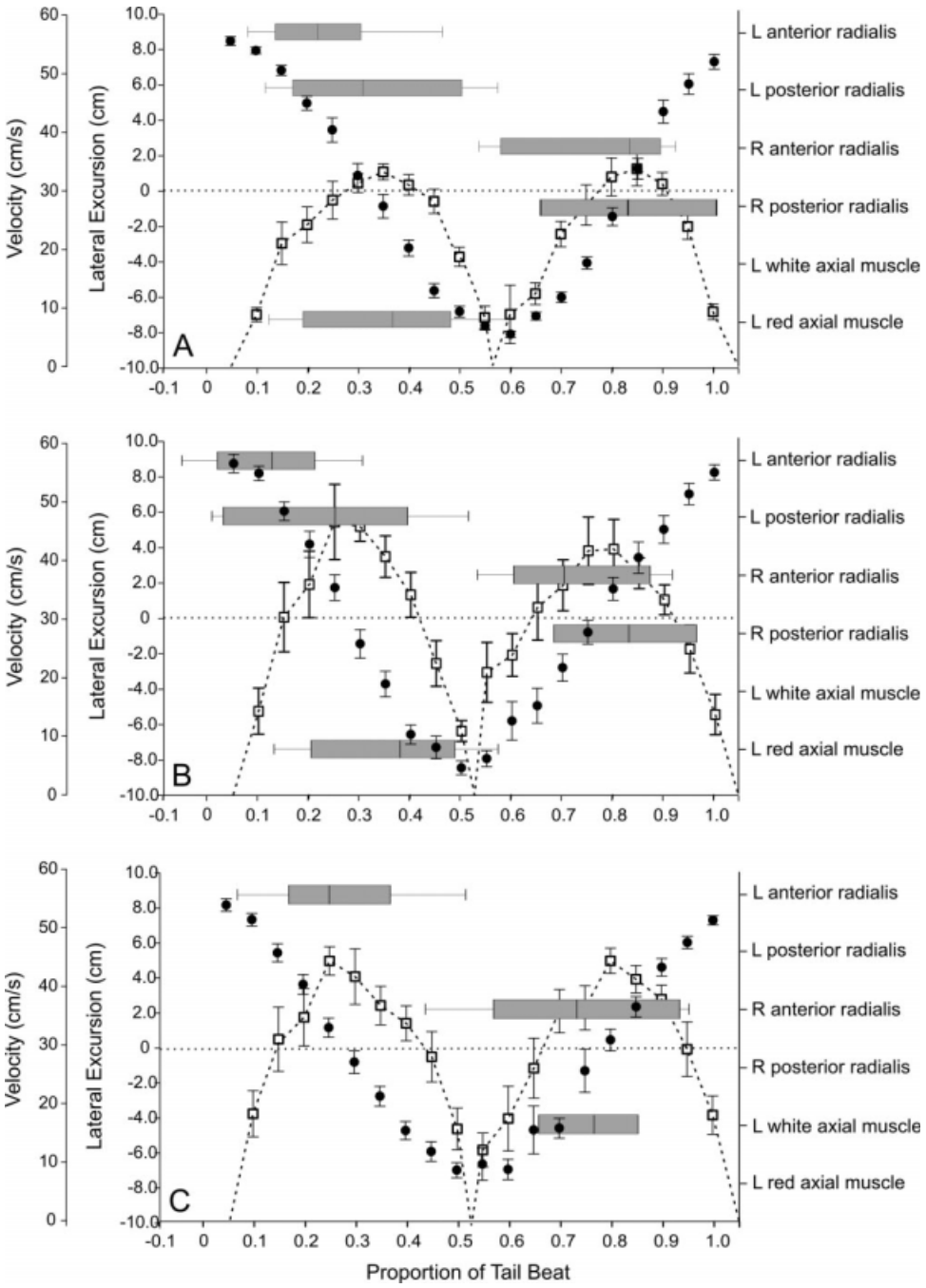

Fig. 5. Summary of electromyographic data and kinematics of the dorsal tip of the tail (point 1) during steady swimming at 0.25 (**A**, $n = 10$), 0.5 (**B**, $n = 8$), and 0.75 L s^{-1} (**C**, $n = 10$). Horizontal bars denote the duration of muscle activity within 75% confidence interval (CI) and error bars denote 95% CI. Lateral excursion of the dorsal tip of the caudal fin (black circles) and mean velocity of the dorsal tip of the tail throughout the tail beat (white squares) are represented as mean and S.E.M.

speeds (Bone, 1966; Bone et al., 1978), which may explain why almost no red muscle activity was observed at the higher speed, of which Bone (1966) reported similar findings in the mid-body axial muscles of sharks. The relative size of the shark may also be a factor, as the critical swimming velocity (U_{crit}, the maximum aerobically sustainable swimming speed) is species–specific and can vary inversely with body size (Graham et al., 1990; Lowe, 1996) and the individuals in this study were large, adult spiny dogfish. In addition, the length of time these sharks were held in captivity may have had an effect on their physical fitness. The inability of the sharks in this study to swim consistently at speeds greater than 0.75 L s^{-1}, in addition to the lack of red muscle activity, supports

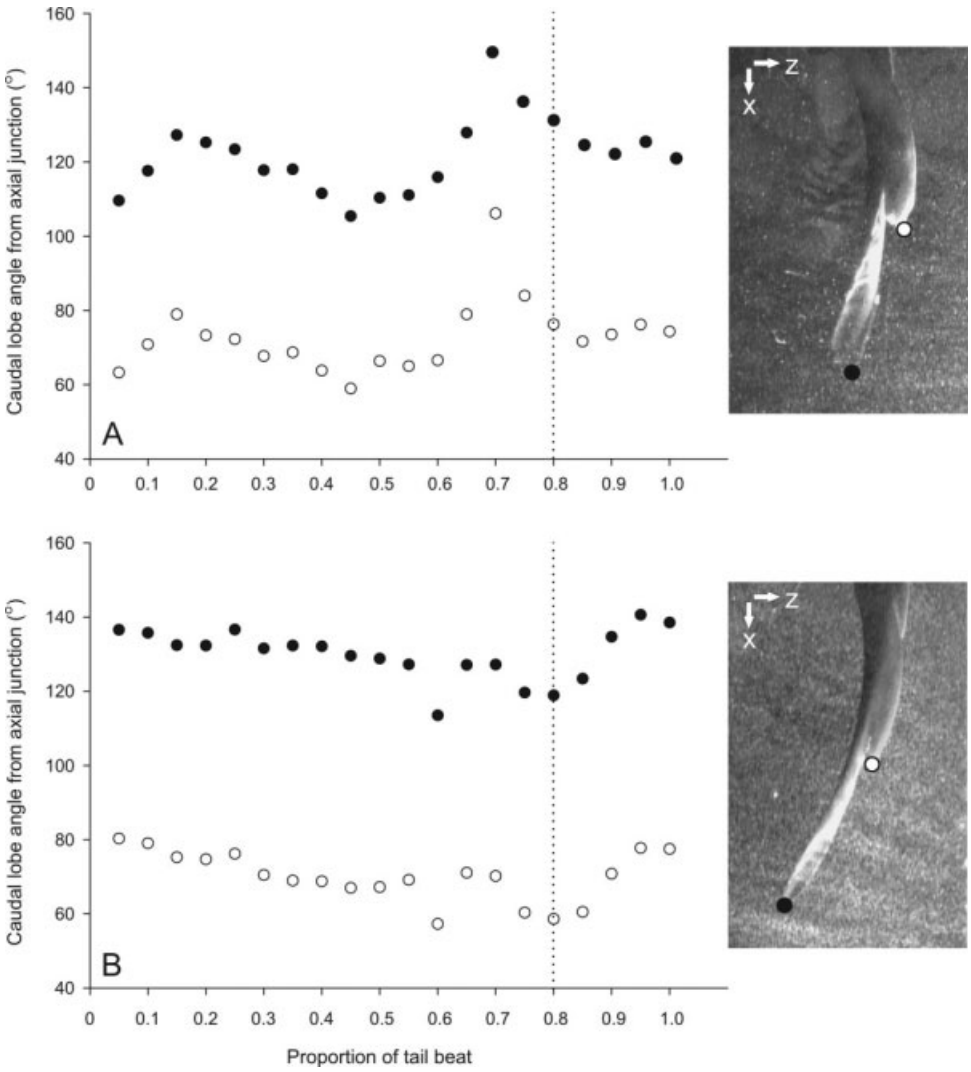

Fig. 6. Angle, in degrees (°), of the three-dimensional position of the dorsal (black circles) and ventral (white circles) tips of the caudal fin relative to the junction of the caudal fin at the peduncle, perpendicular to the long axis of the body during a tail beat, as explained in Fig. 1B. **A:** Steady swimming at 0.5 L s^{-1}. **B:** Steady swimming at 0.75 L s^{-1}. The vertical dotted line at 80% of the tail beat marks the time at which the images (in the ventral view) to the right were captured.

the assumption that they were swimming near or above their U_{crit} and may have been relying on anaerobic fast-glycolytic white muscle contractions. It is possible that the size of the sharks relative to the size of the flow tank restricted their swimming preference to under 1.0 L s^{-1}, but this does not explain the change in activation from red to white muscle tissue. Finally, electrodes in this study were placed farther posteriorly than for previous studies, in the caudal peduncle, which may be affected by more variable muscle activation patterns than would be observed more anteriorly in the body.

Modulation of Kinematics

To swim at increasing speeds, sharks modified tail beat kinematics (see Fig. 5) and not radialis muscle activity duration, relative onset of muscle activity, or muscle EMG burst intensity (see Fig. 4). This suggests that the radialis muscle is not directly involved in modifying tail beat kinematics. At lower swimming speeds, 0.25–0.5 L s^{-1}, maximum velocity of the tail increased with increasing swimming speed while mean frequency increased by only 0.08 Hz and amplitude of the tail beat remained constant. The range of frequencies of tail beats overlapped for sharks swimming at 0.25–0.5 L s^{-1}, suggesting that frequency modulation of swimming speed may occur routinely at slower speeds. Also, the maximum velocity of the tail while the shark swam at 0.5 L s^{-1} had the greatest standard error, which reinforces the likelihood that kinematics were being constantly modified and there is no constraint for a constant pattern of kinematics to maintain a swimming speed. To increase swimming speed by

$\sim$15 cm s^{-1} between 0.5 and 0.75 L s^{-1}, sharks increased tail beat frequency by 0.26 Hz but did not modify velocity or amplitude of the tail. This is not surprising, as sharks modulate frequency, tail beat amplitude, and body wavelength, or combinations of such kinematic parameters to enhance swimming performance (Webb and Keyes, 1982; Graham et al., 1990; Lowe, 1996). However, these results differ from the typical increase in frequency and amplitude observed with increasing speed of swimming in bony fishes (Bainbridge, 1958; Lighthill, 1969; Lauder and Tytell, 2006; Flammang and Lauder, 2008). Unlike bony fishes, sharks possess proprioceptive stretch receptors which are sensitive to the frequency and amplitude of body and fin flexion (Fessard and Sand, 1937; Roberts, 1969; Bone and Chubb, 1976; Bone, 1978); this additional sensory input relaying the position of the caudal fin lobes may trigger modification of fin kinematics in ways different from that in bony fishes.

The increase in swimming speed from 0.5 to 0.75 L s^{-1} also resulted in a reduction of the curvature of the tail fin (see Fig. 6), though some cupping, but to a lesser degree, is observed at higher speeds. The radialis muscle may modulate fin shape at slower swimming speeds and induce cupping, but this seems unlikely as no shape changes were observed during stimulation experiments and the complex interwoven stratum compactum would inhibit direct force transmission from the contracting fibers to cause bending of the ceratotrichia. In addition, ceratotrichia, which are bundles of collagen fibers embedded in a dense tissue matrix (Kemp, 1977) are a very different arrangement from the fin rays of bony fishes in which two hemitrichs can slide relative to each other to bend or stiffen the fin ray against hydrodynamic loading (Montes et al., 1982; Geerlink and Videler, 1987; Alben et al., 2007). In a dead spiny dogfish, the dorsal and ventral lobes of the tail fold backward away from the direction of movement when the tail is manually oscillated in water. The dorsal and ventral lobes of the tail must be actively stiffened, even at slower swimming speeds, in order to prevent the lobes from yielding to hydrodynamic pressure and folding backwards. At higher speeds, activity of the white axial myomeres is rapidly propagated posteriorly on the contralateral side (Figs. 4 and 5), which could stiffen the side of the tail opposite the active radialis muscles and explain the reduction in cupping of the tail fin.

Hypothesized Function of the Radialis Muscle

Relative timing of radialis muscle activity during the tail beat also suggests active stiffening of the dorsal and ventral lobes of the tail. Undulatory swimming in fishes is accomplished by an anterior to posterior wave of muscle activation and contraction (Altringham et al., 1993; Jayne and Lauder, 1995; Shadwick et al., 1998). Activity of the radialis muscle preceded the activity of the axial myomeres of the caudal peduncle, suggesting separate functions and control for the two types of muscles. Assuming a constant propulsive wave velocity of muscle activation, the anterior portion of the radialis, located at 0.84 L, would have the same onset time as the myomeres at $\sim$0.70 L, near the second dorsal fin. Radialis muscle activity, particularly when the anterior and posterior portions were active simultaneously, coincided with periods of greatest velocity of the dorsal tip of the tail during the tail beat (see Fig. 5). Drag is proportional to the square of velocity; therefore, the radialis muscles were active when maximum hydrodynamic drag on the tail occurred.

The anatomical position of the radialis muscle with regards to the collagen fibers of the stratum compactum presents a situation for a stiffening mechanism not previously explored in fish fins. Previous authors have discussed how helically-wound collagen fibers in the skin of sharks adds mechanical support, prevents torsion, and increase mechanical advantage by acting as an exotendon (Motta, 1977; Wainwright et al., 1978; Alexander, 1987; Martinez et al., 2003, 2004; Lingham-Soliar, 2005). However, this earlier research focused on the body of the shark as a whole and measured intramuscular pressure or used beam theory applied to a helically-wound cylinder or ellipse. No specific causative evidence has been produced for the origin of the variations in intramuscular pressure. A common argument against the use of intramuscular pressure in this setting is that it is difficult to determine if increases in measured pressure are hydrostatic or are mechanically induced by the surrounding tissue. By using electromyography, in the much simpler system of the radialis muscle, it is now clear that this muscle is dynamically active, exhibiting speed-variable activation patterns without producing substantial modulation of the fin shape. Instead, as muscles are isovolumetric, isometric contraction of the radialis muscle fibers may cause concurrent bulging of the fibers laterally, putting pressure on the superficial stratum compactum (Brainerd and Azizi, 2005), as well as transferring force to the deepest layer of collagen fibers onto which the radialis muscle fibers insert directly. Preliminary research combining electromyography, sonomicrometry, and intramuscular pressure measurements of the radialis muscle supports the hypothesis that radialis muscle activity results in an increase in intramuscular pressure and a concurrent lateral expansion that is transferred to the dermis; however, a larger sample size is needed to confirm these results (Flammang, unpublished). Stiffening of the shark

tail appears to be accomplished solely by the radialis at slower swimming speeds, as inferred from electromyographic and kinematic analyses. At higher speeds, the contralateral activity of white axial muscle in the tail would create additional pressure laterally, resulting in the tail becoming even stiffer than when the radialis is active alone. Consequently, the tail should be stiffer at higher speeds and exhibit less cupping. This is certainly not the first instance of hydrostatic pressure used for stiffening in vertebrates; it is also known to occur in the tails of tadpoles (Doherty et al., 1998; Koehl et al., 2000), fishes (Hebrank, 1980; Long and Nipper, 1996; Long et al., 1996; Westneat et al., 1998), and cetaceans (Pabst, 1996a,b; Hamilton et al., 2004), among others. However, this may be the first instance of localized control of stiffness by a specialized muscle that interacts directly with the stratum compactum.

ACKNOWLEDGMENTS

The author is indebted to Emanuel Azizi for patience and assistance during a pilot study of this research at Friday Harbor Laboratories (University of Washington, USA) in 2005, to Rachel Strauss and Jasmine Edo for assistance in digitizing videos, Andy Williston for photography assistance, Karsten Hartel for assistance with the Harvard MCZ fish collection, Woods Hole Oceanographic Institute Marine Resource Center for specimens, and to the members of the Lauder laboratory (Harvard University) for insightful discussions and comments on an earlier version of this manuscript. All sharks were handled ethically according to Harvard University Institutional Animal Care and Use Committee guidelines, protocol #20-03.

LITERATURE CITED

Affleck RJ. 1950. Some points in the function, development and evolution of the tail in fishes. Proc Zool Soc Lond 120:349–368.

Alben S, Madden PGA, Lauder GV. 2007. The mechanics of active fin-shape control in ray-finned fishes. J R Soc Inter 4:243–256.

Alexander RM. 1965. The lift produced by the heterocercal tails of selachii. J Exp Biol 43:131–138.

Alexander RM. 1987. Bending of cylindrical animals with helical fibres in their skin or cuticule. J Theor Biol 124:97–110.

Altringham JD, Wardle CS, Smith CI. 1993. Myotomal muscle function at different locations in the body of a swimming fish. J Exp Biol 182:191–206.

Bainbridge R. 1958. The speed of swimming of fish as related to size and to the frequency and amplitude of the tail beat. J Exp Biol 35:109–133.

Bone Q. 1966. On the function of the two types of myotomal muscle fibre in elasmobranch fish. J Mar Biol Assoc UK 46:321–349.

Bone Q. 1978. Locomotor muscle. In: Hoar WS, Randall DJ, editors. Fish Physiology Vol VII Locomotion. New York: Academic Press. pp 361–424.

Bone Q. 1999. Muscular system: Microscopical anatomy, physiology, and biochemistry of elasmobranch muscle fibers. In: Hamlett WC, editor. Sharks, Skates, and Rays: The Biology of Elasmobranch Fishes. Baltimore, MD: Johns Hopkins University Press. pp 115–143.

Bone Q, Chubb AD. 1976. On the structure of the corpuscular proprioceptive endings in sharks. J Mar Biol Assoc UK 56:925–928.

Bone Q, Kiceniuk J, Jones DR. 1978. On the role of the different fibre types in fish myotomes at intermediate swimming speeds. Fish Bull 76:691–699.

Bone Q, Johnston IA, Pulsford A, Ryan KP. 1986. Contractile properties and ultrastructure of three types of muscle fibre in the dogfish myotome. J Muscle Res Cell Motil 7:47–56.

Brainerd EL, Azizi E. 2005. Muscle fiber angle, segment bulging and architectural gear ratio in segmented musculature. J Exp Biol 208:3249–3261.

Dickson KA, Gregorio MO, Gruber SJ, Loefler KL, Tran M, Terrell C. 1993. Biochemical indices of aerobic and anaerobic capacity in muscle tissues of California elasmobranch fishes differing in typical activity level. Mar Biol 117:185–193.

Doherty PA, Wassersug RJ, Lee JM. 1998. Mechanical properties of the tadpole tail fin. J Exp Biol 201:2691–2699.

Domenici P, Standen EM, Levine RP. 2004. Escape manoeuvres in the spiny dogfish (*Squalus acanthias*). J Exp Biol 207:2339–2349.

Donley JM, Shadwick RE. 2003. Steady swimming muscle dynamics in the leopard shark *Triakis semifasciata*. J Exp Biol 206:1117–1126.

Donley JM, Shadwick RE, Sepulveda CA, Konstantinidis P, Gemballa S. 2005. Patterns of red muscle strain/activation and body kinematics during steady swimming in a lamnid shark, the shortfin mako (*Isurus oxyrinchus*). J Exp Biol 208:2377–2387.

Douady CJ, Dosay M, Shivji MS, Stanhope MJ. 2003. Molecular phylogenetic evidence refuting the hypothesis of Batoidea (rays and skates) as derived sharks. Mol Phylogenet Evol 26:215–221.

Ebert DA. 2003. Sharks, Rays, and Chimaeras of California. California: University of California Press. p 284.

Ferry LA, Lauder GV. 1996. Heterocercal tail function in leopard sharks: A three-dimensional kinematic analysis of two models. J Exp Biol 199:2253–2268.

Fessard A, Sand A. 1937. Stretch receptors in the muscles of fishes. J Exp Biol 14:383–404.

Flammang BE, Lauder GV. 2008. Speed-dependent intrinsic caudal fin muscle recruitment during steady swimming in bluegill sunfish, *Lepomis macrochirus*. J Exp Biol 211:587–598.

Flammang BE, Lauder GV. 2009. Caudal fin shape modulation and control during acceleration, braking and backing maneuvers in bluegill sunfish, *Lepomis macrochirus*. J Exp Biol 212:277–286.

Geerlink PJ, Videler JJ. 1987. The relation between structure and bending properties of teleost fin rays. Nether J Zool 37:59–80.

Gemballa S. 2004. The musculoskeletal system of the caudal fin in the basal Actinopterygii: Heterocercy, diphycercy, homocercy. Zoomorphology 123:15–30.

Graham JB, Dewar H, Lai NC, Lowell WR, Arce SM. 1990. Aspects of shark swimming performance determined using a large water tunnel. J Exp Biol 151:175–192.

Greer-Walker M, Pull GA. 1975. A survey of red and white muscle in marine fish. J Fish Biol 7:295–300.

Hamilton JL, Dillaman RM, McLellan WA, Pabst DA. 2004. Structural fiber reinforcement of keel blubber in Harbor porpoise (*Phocoena phocoena*). J Morphol 261:105–117.

Hebrank MR. 1980. Mechanical properties and locomotor functions of eel skin. Biol Bull 158:58–68.

Hedrick TL. 2008. Software techniques for two- and three-dimensional kinematic measurements of biological and biomimetic systems. Bioinspir Biomim 3:034001–034006.

Jayne BC, Lauder GV. 1995. Red muscle motor patterns during steady swimming in largemouth bass: Effects of speed and correlations with axial kinematics. J Exp Biol 198:1575–1587.
Kemp NE. 1977. Banding pattern and fibrillogenesis of ceratotrichia. J Morphol 154:187–204.
Koehl MAR, Quillin KJ, Pell CA. 2000. Mechanical design of fiber-wound hydraulic skeletons: The stiffening and straightening of embryonic notochords. Am Zool 40:28–41.
Lauder GV, Tytell ED. 2006. Hydrodynamics of undulatory propulsion. In: Shadwick RE, Lauder GV, editors. Fish Physiology. San Diego: Academic Press. p 425.
Lighthill MJ. 1969. Hydrodynamics of aquatic animal propulsion. Annu Rev Fluid Mech 1:413–446.
Lingham-Soliar T. 2005. Caudal fin in the White shark. Carcharadon carcharius (Lamnidae): A dynamic propeller for fast, efficient, swimming. J Morphol 264:233–252.
Long J, Hale ME, McHenry MJ, Westneat MW. 1996. Functions of fish skin: Flexural stiffness and steady swimming of longnose gar, *Lepisosteus osseus*. J Exp Biol 199:2139–2151.
Long JH, Nipper KS. 1996. The importance of body stiffness in undulatory propulsion. Am Zool 36:678–694.
Lowe CG. 1996. Kinematics and critical swimming speed of juvenile scalloped hammerhead sharks. J Exp Biol 199:2605–2610.
Lowndes AG. 1955. Density of fishes: Some notes on the swimming of fish to be correlated with density, sinking factor, and the load carried. Ann Mag Nat Hist 8:241–256.
Martinez G, Drucker EG, Summers AP. 2003. Under pressure to swim fast: Intramuscular pressure of free swimming sharks. Integr Comp Biol 42:1273.
Masuda H, Allen GR. 1993. Meeresfische der Welt–Grob-Indopazifische Region. Herrenteich, Melle: Tetra Verlag.
Montes GS, Becerra J, Toledo OMS, Gordilho MA, Junqueira LCU. 1982. Fine structure and histochemistry of the tail fin ray in teleosts. Histochemistry 75:363–376.
Motta PJ. 1977. Anatomy and functional morphology of dermal collagen fibers in sharks. Copeia 1977:454–464.
Nursall JR. 1958. The caudal fin as a hydrofoil. Evolution 12:116–120.
Pabst DA. 1996a. Morphology of the subdermal connective sheath of dolphins: A new fiber-wound, thin-walled, pressurized cylinder model for swimming vertebrates. J Zool Lond 238:35–52.
Pabst DA. 1996b. Springs in swimming animals. Am Zool 36:723–735.
Roberts BL. 1969. The response of a proprioceptor to the undulatory movements of a dogfish. J Exp Biol 51:775–785.
Sepulveda CA, Wegner NC, Bernal D, Graham JB. 2005. The red muscle morphology of the thresher sharks (family Alopiidae). J Exp Biol 208:4255–4261.
Shadwick RE, Steffensen JF, Katz SL, Knower T. 1998. Muscle dynamics in fish during steady swimming. Am Zool 38:755–770.
Shirai S. 1996. Phylogenetic interrelationships of Neoselachians (Chondrichthyes: Euselachii). In: Stiassny MLJ, Parenti LR, Johnson GD, editors. Interrelationships of Fishes. San Diego: Academic Press, Inc. pp 9–34.
Simons JR. 1970. The direction of the thrust produced by the heterocercal tails of two dissimilar elasmobranchs: The Port Jackson shark. Heterodontus portusjacksoni (Meyer), and the piked dogfish, *Squalus megalops* (Macleay). J Exp Biol 52:95–107.
Wainwright SA, Vosburgh F, Hebrank JH. 1978. Shark skin: Function in locomotion. Science 202:747–749.
Webb PW, Keyes RS. 1982. Swimming kinematics in sharks. Fish Bull 80:803–812.
Westneat MW, Hale ME, McHenry MJ, Long JH Jr. 1998. Mechanics of the fast-start: Muscle function and the role of intramuscular pressure in the escape behavior of *Amia calva* and *Polypterus palmas*. J Exp Biol 201:3041–3055.
Wetherbee BM, Gruber SJ, Cortes E. 1990. Diet, feeding habits, digestion, and consumption in sharks, with special reference to the lemon shark, *Negaprion brevirostris*. In: Pratt HL Jr, Gruber SJ, Taniuchi T, editors. Elasmobranchs as Living Resources: Advances in the Biology, Ecology, Systematics, and the Status of the Fisheries NOAA Tech Rep NMFS 90. pp 29–47.
Wilga CD, Lauder GV. 2002. Function of heterocercal tail in sharks: Quantitative wake dynamics during steady swimming and vertical maneuvering. J Exp Biol 205:2365–2374.
Wilga CD, Lauder GV. 2004. Hydrodynamic function of the shark's tail. Nature 430:850.